Role of metallothionein in nitric oxide signaling as revealed by a green fluorescent fusion protein

Linda L. Pearce*†, Robin E. Gandley†‡, Weiping Han*, Karla Wasserloos*, Molly Stitt*, Anthony J. Kanai*, Margaret K. McLaughlin‡, Bruce R. Pitt*, and Edwin S. Levitan*§

Department of *Pharmacology and ‡Department of Obstetrics, Gynecology, and Reproductive Sciences, University of Pittsburgh School of Medicine, Pittsburgh, PA 15261

Edited by Roger Y. Tsien, University of California, San Diego, La Jolla, CA, and approved November 8, 1999 (received for review July 12, 1999)

Although the function of metallothionein (MT), a 6- to 7-kDa cysteine-rich metal binding protein, remains unclear, it has been suggested from *in vitro* studies that MT is an important component of intracellular redox signaling, including being a target for nitric oxide (NO). To directly study the interaction between MT and NO in live cells, we generated a fusion protein consisting of MT sandwiched between two mutant green fluorescent proteins (GFPs). *In vitro* studies with this chimera (FRET-MT) demonstrate that fluorescent resonance energy transfer (FRET) can be used to follow conformational changes indicative of metal release from MT. Imaging experiments with live endothelial cells show that agents that increase cytoplasmic Ca^{2+} act via endogenously generated NO to rapidly and persistently release metal from MT. A role for this interaction in intact tissue is supported by the finding that the myogenic reflex of mesenteric arteries is absent in MT knockout mice ($MT^{-/-}$) unless endogenous NO synthesis is blocked. These results are the first application of intramolecular green fluorescent protein (GFP)-based FRET in a native protein and demonstrate the utility of FRET-MT as an intracellular surrogate indicator of NO production. In addition, an important role of metal thiolate clusters of MT in NO signaling in vascular tissue is revealed.

Metallothioneins (MT) are 6- to 7-kDa intracellular cysteine-rich (30 mol%) metal binding proteins whose function remains elusive (1). A critical role for MT in protection against toxic non-essential metals such as cadmium is apparent (2), and MT appears to act as an antioxidant under a variety of conditions (3). More recently, *in vitro* data support the hypothesis that MT is a critical link between cellular redox state and metal ion homeostasis (4–6). In this regard, cysteines of metal thiolate clusters confer unique redox sensitivity to an otherwise redox inert metal ligand (e.g., zinc) and facilitate the potential for MT to participate in intracellular signal transduction pathways (7). In the current study, we examine this latter novel hypothesis in intact cells and tissue.

We chose to study the interaction of MT and the free radical, nitric oxide (NO), because (*i*) the bioregulatory targets of NO usually contain cysteines and/or metals at their active or allosteric site (8); (*ii*) NO (or a secondary product) reacts with MT *in vitro*, leading to the release of zinc (9) or cadmium (10); (*iii*) NO can form stable EPR-detectable complexes with MT *in vitro* (11); and (*iv*) MT can reduce the sensitivity of cells to potential toxic levels of NO (12). Application of a chimeric construct (called FRET-MT) based on a recently described cameleon for calmodulin (13) revealed an NO-induced conformational change in MT, indicative of metal release, thereby providing the first demonstrations of (*i*) changes in intramolecular FRET (fluorescence resonance energy transfer) of a native protein; and (*ii*) metal release from MT in response to physiologic stimuli in intact cells. Furthermore, the lack of myogenic reflex in superior mesenteric arteries of $MT^{-/-}$ mice and its restoration after inhibition of nitric oxide synthase reveal an important role for metal thiolate clusters in NO signaling in vascular tissue.

Materials and Methods

Tissue Culture and MT Knockout Mice. Chinese hamster ovary cells were obtained from American Type Culture Collection and were grown in Ham's F-10 medium supplemented with 10% fetal calf serum, 100 units/ml penicillin, and 100 μg/ml streptomycin. Sheep pulmonary artery endothelial cells (SPAEC) were cultured from sheep pulmonary arteries, obtained from a nearby slaughterhouse, as described (14). SPAEC were grown in Opti-Mem supplemented with 10% fetal bovine serum supplemented with endothelial cell growth supplement (15 μg/ml), 10 units/ml heparin sulfate, 100 units/ml penicillin, and 100 μg/ml streptomycin at 37°C in an atmosphere with 5% CO_2.

We imported breeding pairs of MT-I- and -II-deficient ($MT^{-/-}$) mice from Michalska and Choo (15). The mice are on a mixed genetic background of OLA129 and C57BL6 strains. We bred $MT^{-/-}$ with C57BL6 mice obtained from The Jackson Laboratory to generate a parental heterozygous chimera that in turn was backbred to the C57BL6 wild type. This backbreeding resulted in ≈50% offspring that were heterozygous mutants. These mutants were identified by a genotyping protocol using PCR-based restriction digestion strategy on novel sites within a murine MT-II gene that was mutated. An additional round of interbreeding and genotyping resulted in F2 generation of $MT^{-/-}$ and $MT^{+/+}$ mice that allowed establishment of breeding colonies in which the genetic contributions of the two strains were assumed to be similar. An additional wild-type control consisting of the offspring of breeding of OLA129 and C57BL6 was also tested. Mice were kept in specific-pathogen-free animal housing. All experiments were performed with male mice between 8 and 18 weeks of age.

Gene Construction. The cDNA for yellow cameleon-2 (containing ECFP and EYFP) (13) was kindly provided by Roger Tsien (University of California, San Diego), and the cDNA for human metallothionein IIa (hMTIIa) was received from Jan Vilcek (New York University Medical Center). Two restriction sites (*Sph*I and *Sac*I) were introduced by PCR into the 5′ and 3′ ends of the hMTIIa cDNA. The hMTIIa PCR product was ligated in frame into a pSP72 yellow cameleon-2 subclone after excision of CAM-M13 cDNA with *Sph*I and *Sac*I restriction enzymes. The ECFP-hMTIIa-EYFP *Hin*dIII/*Eco*RI restriction product was then subcloned into the mammalian expression vector pcDNA3.1(+) (Invitrogen). Controls were performed on occasion with either cDNA for yellow cameleon-2 or plasmid containing cDNA for bacterial β-galactosidase driven by cytomegalovirus promoter.

This paper was submitted directly (Track II) to the PNAS office.

Abbreviations: GFP, green fluorescent protein; FRET, fluorescence resonance energy transfer; MT, metallothionein; NO, nitric oxide; SPAEC, sheep pulmonary artery endothelial cell; eNOS, endothelial nitric oxide synthase; L-NAME, L-nitro-arginine-methyl-ester.

§To whom reprint requests should be addressed at: E1351 Biomedical Science Tower, Department of Pharmacology, University of Pittsburgh, Pittsburgh, PA 15261. E-mail: levitan@server.pharm.pitt.edu.

†L.L.P. and R.E.G. contributed equally to this work.

The publication costs of this article were defrayed in part by page charge payment. This article must therefore be hereby marked "*advertisement*" in accordance with 18 U.S.C. §1734 solely to indicate this fact.

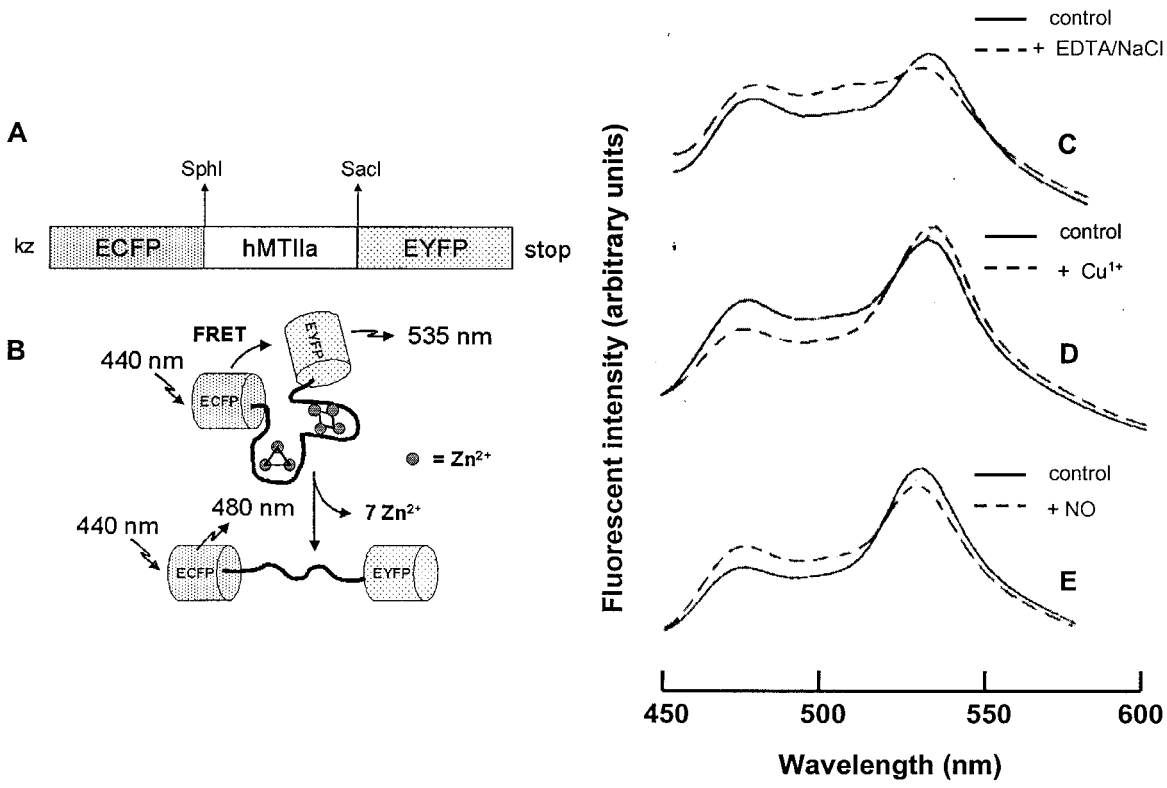

Fig. 1. (*A*) Properties of FRET-MT. Shown is FRET-MT cDNA construct of human type IIa metallothionein (hMTIIAa), flanked by enhanced cyan fluorescent protein (ECFP) and enhanced yellow fluorescent protein (EYFP). (*B*) Scheme of the above construct (FRET-MT) showing possible unfolding, metal release and consequent changes in FRET induced by EDTA/NaCl. (*C–E*) Fluorescent emission spectra of lysates as isolated (control) and after addition of 1 mM EDTA/150 mM NaCl (decrease in 535 nm intensity and increase in 480 nm intensity after 8-h incubation) (*C*); 50 μM Cu^{1+} (immediate decrease in 480 nm intensity and increase in 535 nm intensity) (*D*); and 100 μM of NO (immediate decrease in 535 nm intensity and increase in 480 nm intensity) (*E*).

***In Vitro* Spectroscopy.** One to four days after cDNA transfection with Lipofectamine Plus (GIBCO/BRL), Chinese hamster ovary cells (≈7 million) were harvested, were lysed by sonication, and were spun at 10,000 × *g*. The supernatant was resuspended in Tris (Tris[hydroxymethyl]aminomethane) buffer (pH 7.4), and fluorescent emission measurements were performed by using a SLM–Aminco (Urbana, IL) SPF 500C spectrofluorometer with an excitation wavelength of 430 nm under aerobic conditions.

Imaging. Two to four days after cDNA transfection with Lipofectamine Plus (GIBCO/BRL), SPAECs were imaged on a Nikon inverted microscope with a Photometrics cooled charge-coupled device camera (Tucson, AZ) controlled by ISEE software (Inovision, Raleigh, NC). The dual emission imaging was accomplished by using a 440DF20 excitation filter, a 455 DRLP dichroic mirror, and alternating emission filters (480DF30 for ECFP, 535DF25 for EYFP). For each experiment, images were collected at room temperature from a minimum of five cells from at least two different cell preparations. Cells were bathed in a normal saline solution consisting of 140 mM NaCl, 0.8 mM $MgCl_2$, 10 mM Hepes (4-(2-hydroxyethyl)-1-piperazineethanesulfonic acid), 5.4 mM KCl, 5 mM $CaCl_2$, and 10 mM glucose at pH 7.4. All imaging experiments were performed under aerobic conditions.

Amperometric NO Measurements. A Nafion-coated porphyrinic microsensor (tip diameter, 5–15 μm; response time, 1 ms; detection limit, 1 nM NO) was positioned on individual cells as described (16).

Pressurized Arteriograph and Myogenic Reactivity. Mesenteric resistance arteries [diameters of 200–250 microns at 60 mmHg (1 mmHg = 133 Pa)] were removed from wild-type and MT knockout mice. Vessels were mounted on glass cannulae in pairs (one wild type; one null mutant) in a dual chamber pressurized arteriograph. The arteriograph was placed on the stage of a compound microscope. The proximal cannula was joined in series with a pressure transducer connected to a servo-controlled peristaltic pump. This allowed a desired intraluminal pressure to be established, maintained, and recorded in the absence of flow. The vessels were maintained in Hepes-buffered salt solution and were equilibrated for 1 h at 60 mmHg. At 45 min into the equilibrium, a conditioning stretch was performed from 60 to 100 mmHg. A video camera on the microscope provided an image of the artery on a television monitor, and measurements of lumen diameter and wall thickness were continuously made by using a video dimension analyzer (17). Myogenic tone was assessed by decreasing the intraluminal pressure to 20 mmHg for 10 min, after which pressure was rapidly (2 s) increased by 20 mmHg at 4-min intervals up to 120 mmHg. L-nitro-arginine-methyl-ester (L-NAME) (0.25 mM) was added to the bath to inhibit nitric oxide synthase for 15 min before repeating the changing pressure protocol. To reverse inhibition of nitric oxide synthase, L-arginine was given at a concentration of 2.5 mM for 15 min, and the protocol was repeated. The smooth muscle was then inactivated in a solution of calcium-free Hepes saline solution with papaverine (0.1 mM) and ethylene-bis(oxyethylenenitrilo)tetraacetic acid (EGTA), and the protocol was repeated. Percent tone was calculated as $[(D_r - D_{pss})/D_r] \times 100$, where D_r is the passive (smooth muscle inactivated) diameter

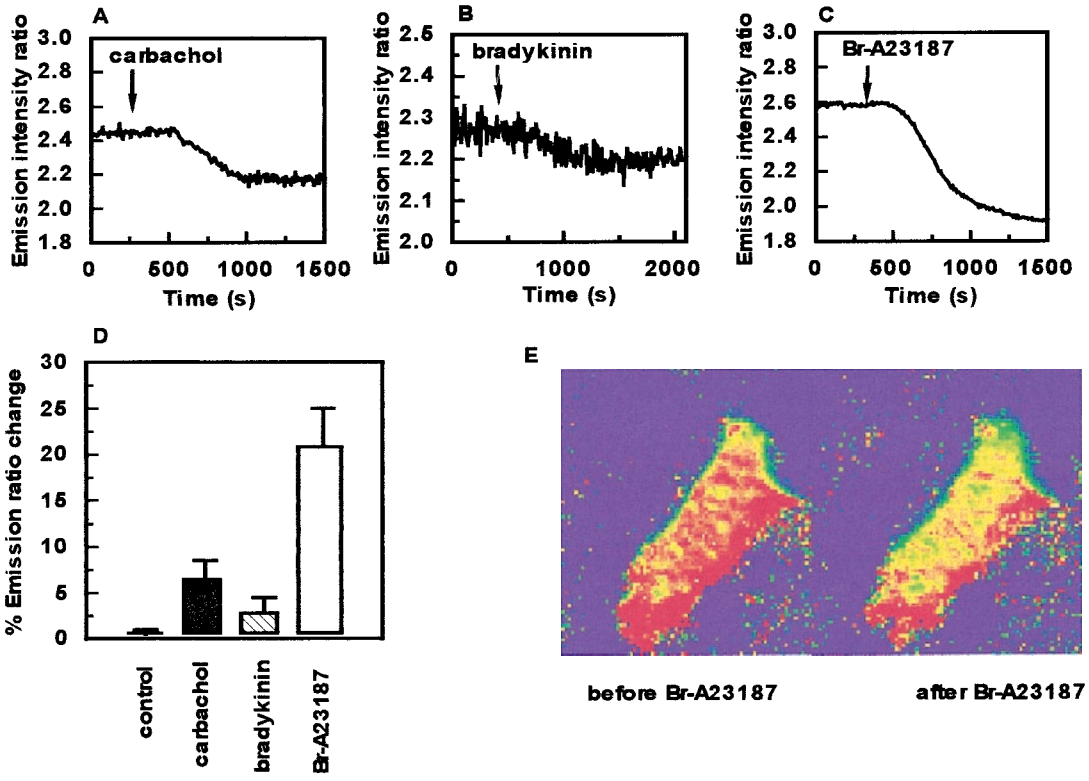

Fig. 2. Regulation of FRET-MT function in endothelial cells. Emission intensity ratio (535 nm/480 nm) changes over time after addition of 10 μM carbachol (indicated by arrow) (*A*); 20 μM bradykinin (indicated by arrow) (*B*); or 1 μM of the calcium ionophore Br-A23187 (indicated by arrow) (*C*). (*D*) Histogram of percent emission ratio changes showing control (time, 2,000 s), carbachol, bradykinin, and Br-A23187 with relative error bars. (*E*) Pseudo-color representation of a SPAEC before and after addition of Br-A23187.

and D_{pss} is the internal diameter in buffered saline solution at each pressure.

Results

FRET-MT, *in Vitro*. Following the example of the Ca^{2+} indicator, cameleon-2 (13), a cyan green fluorescent protein (GFP) variant (ECFP) and a yellow GFP variant (EYFP) were fused to the amino and carboxyl termini of MT, respectively (Fig. 1*A*). The combination of the 6-kDa MT with two 27-kDa GFPs resulted in the formation of a 60-kDa fusion protein (called FRET-MT) as determined by SDS/PAGE analysis and Western blotting of transfected Chinese hamster ovary cell lysates. Cd^{2+} saturation assays were performed on lysates from FRET-MT-transfected and lacZ-transfected cells (18). Even though only a fraction of the cells expressed FRET-MT, an increased amount of bound $^{109}Cd^{2+}$ was found with FRET-MT lysates (0.27 ± 0.04 μg of Cd^{2+}/mg of protein) compared with control lysates (0.07 ± 0.01 μg of Cd^{2+}/mg of protein) ($n = 5$, $P < 0.05$). Therefore, FRET-MT retains MT's ability to bind metal ions.

The cyan and yellow GFPs can act as donor and acceptor for FRET and hence reveal changes in intramolecular proximity and relative orientation of the fluorophores (19, 20). These changes are schematically shown in Fig. 1*B* for the release of zinc ions from FRET-MT. In the case of FRET-MT, fluorescent emission spectra indicate that FRET can be used to follow metal binding and release by the new construct. For example, it is known that incubation of MT for several hours with the metal chelator ethylenediaminetetraacetic acid (EDTA) and NaCl causes depletion of bound metals and protein unfolding (21). After similar treatment of FRET-MT, the emission ratio that quantifies energy transfer ($F_{535\ nm}/F_{480\ nm}$) dropped from 1.8 to 1.1, indicating that the conformational change that accompanies loss of metals is detectable (Fig. 1*C*). As expected from the known slow metal dissociation, no acute effect of EDTA/NaCl on FRET-MT was observed and no change in emission ratio was found with a control sample of FRET-MT. Furthermore, when Cu^{1+} was added to naive cell lysate, FRET efficiency increased from a ratio of 1.8 to 2.2, indicating that the FRET-MT was not fully saturated and that increased metal binding can also be followed (Fig. 1*D*). Finally, *in vitro* studies of zinc-loaded MT under aerobic conditions have previously shown that NO forms nitrosothiols with MT cysteine groups and induces release of metal ions (9, 10). We found that addition of an aqueous solution of NO to the cell lysate containing FRET-MT decreased the FRET efficiency as expected ($F_{535\ nm}/F_{480\ nm}$ dropped from 1.8 to 1.4) (Fig. 1e). NO did not change FRET efficiency in Ca^{2+}-loaded or Ca^{2+}-free cameleon-2, providing evidence that NO does not directly interact with either the cyan or the yellow fluorophore. Likewise, NO does not affect the fluorescence signal from metal-free FRET-MT. Finally, in contrast to cameleon-2, addition of 100 μM Ca^{2+} to the FRET-MT did not alter energy transfer. Thus, *in vitro* studies establish that FRET-MT can be used to follow conformational changes indicative of metal binding and release.

FRET-MT, NO, and Cultured Endothelial Cells. To determine whether MT can be regulated in living cells, the FRET-MT signal was imaged in live sheep pulmonary artery endothelial cells (SPAECs). We were particularly interested in examining the effects of agents that are known to acutely regulate endothelial cell function. As can be seen in Fig. 2 *A–D*, the muscarinic agonists carbachol, bradykinin, and the Ca^{2+} ionophore Br-A23187 each reduced energy transfer in endothelial cells. Furthermore, changes in fluorescence were uniform throughout the

PHARMACOLOGY

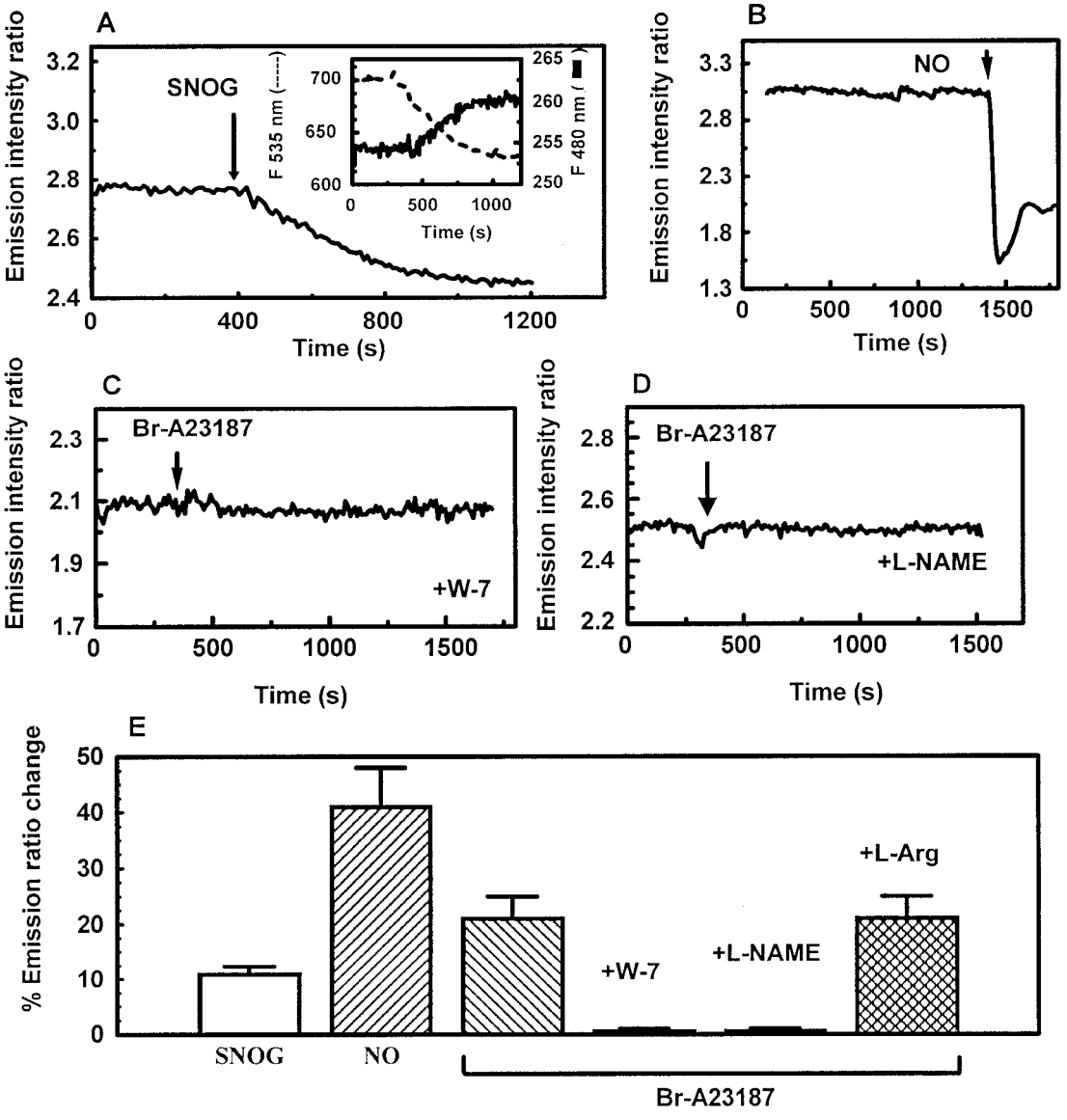

Fig. 3. eNOS-generated NO regulates FRET-MT. Shown are emission ratio changes (535 nm/480 nm) in response to *S*-nitrosylglutathione (100 μM, 100 μM DTT was present throughout the experiment) (*A*) [*Inset* shows individual 535-nm fluorescence intensity (left axis) and 480-nm fluorescence intensity (right axis)]; $\approx$1 mM NO (*B*); 1 μM BrA23187 in the presence of 15 μM W-7 (*C*); and 1 μM BrA23187 in the presence of 1 mM L-NAME using arginine-depleted cells (*D*). (*E*) Histogram of percent emission changes with relative error bars (see text for details).

cytoplasm (Fig. 2*E*). Thus, these results demonstrate that metal binding by MT can be rapidly regulated by activation of endogenous receptors or Ca^{2+} influx in live cells.

Each of these stimuli is known to elevate cytoplasmic Ca^{2+} that in turn activates the calmodulin dependent enzyme endothelial nitric oxide synthase (eNOS). To ascertain whether this mechanism could account for the Ca^{2+} effect on MT, we first tested whether FRET-MT retains its sensitivity to NO when expressed in endothelial cells. Fig. 3*A* shows that the FRET-MT signal from a representative cell decreases in response to bath application of the NO donor *S*-nitrosylglutathione (100 μM) in the presence of dithiotreitol (DTT) (100 μM). This treatment is known to generate a steady state concentration of $\approx$10 μM NO (22). This decrease in FRET persisted for over 10 min after the removal of *S*-nitrosylglutathione from the bath solution (data not shown). Buffer saturated with NO gas added as a bolus resulted in a similar but much larger and rapid decrease in FRET efficiency (Fig. 3*B*), presumably because of the greater concentration of NO ($\approx$1 mM). In this case, there seemed to be a small amount of recovery of the FRET efficiency over time. Importantly, these results demonstrate that NO can still regulate FRET-MT in the cytoplasm of live cells.

We then focused on whether eNOS mediates Ca^{2+}-dependent regulation of MT. First, fluorescence microscopy was carried out on FRET-MT containing endothelial cells in the presence of *N*-(6-aminohexyl)5-chloro-1-napthalenesulfonamide (W-7). W-7 binds to the hydrophobic patch on calmodulin and prevents the activation of Ca^{2+}/calmodulin regulated-enzymes such as eNOS (23). We found that, in contrast to controls, W-7-treated SPAEC did not respond to elevation of cytoplasmic Ca^{2+} (Fig. 3*C*). To further investigate the linkage between the emission ratio changes and NO production, Ca^{2+} levels were increased in FRET-MT containing cells starved of the eNOS substrate L-arginine and incubated with the NOS inhibitor L-NAME. Measurements of extracellular NO levels with a Nafion-coated porphyrinic microsensor (16) verified that this treatment abol-

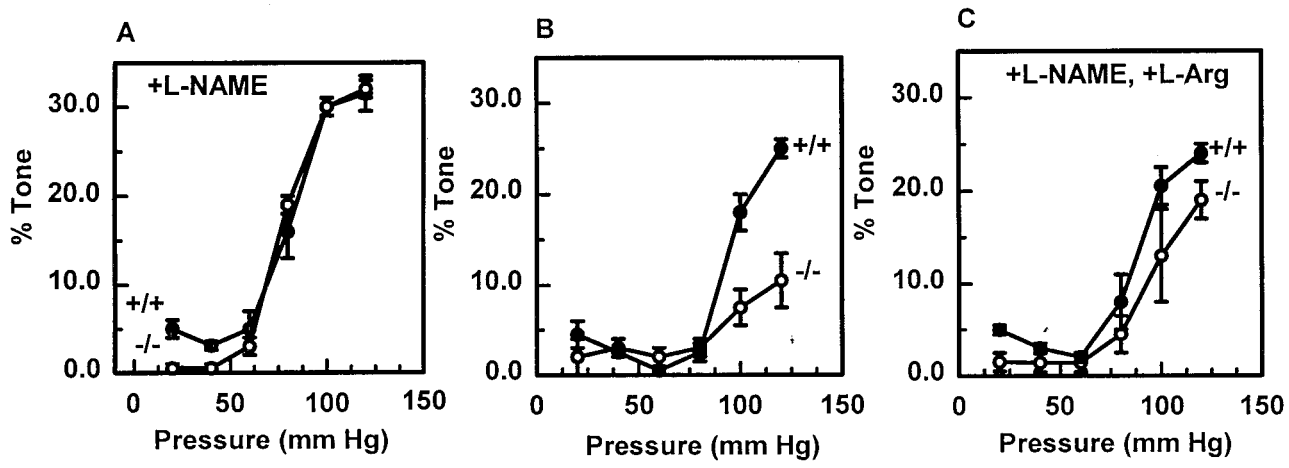

Fig. 4. Lack of myogenic reactivity in mesenteric arteries from $MT^{-/-}$ mice can be restored by inhibition of nitric oxide synthase. The percent myogenic tone (difference between passive diameter and reactive diameter) of mesenteric arteries from $MT^{+/+}$ (closed circles) and $MT^{-/-}$ (open circles) mice ($n = 5$, with relative error bars) was measured with stepwise increases in luminal pressure of 20 mmHg in the presence of L-NAME (*A*), the absence of L-NAME (*B*), and after adding L-arginine after the pretreatment with L-NAME (*D*).

ished NO release induced by the Ca^{2+} ionophore. FRET-MT in these cells also had no response to the elevation of cytoplasmic Ca^{2+} levels (Fig. 3*D*). However, addition of L-arginine and removal of L-NAME rescued electrochemically measured NO release (data not shown) and the change in FRET-MT signal induced by Ca^{2+} (Fig. 3*E*). Thus, the loss of the effect was not an irreversible artifact induced by the treatment. Rather, these data show that the change in MT function induced by Ca^{2+} is mediated by eNOS-generated NO.

Myogenic Reflex, NO, and MT. We then sought to identify a physiologic role for the interaction of MT and endothelial derived NO by examining the myogenic reflex of mesenteric arteries from wild-type ($MT^{+/+}$) and MT knockout ($MT^{-/-}$) mice. There was 0.12 ± 0.01 μg/mg protein MT in $+/+$ vessels and no detectable MT in $-/-$ vessels. Pressurized arteriography and videomicroscopy revealed no difference between the diameter pressure curves of vessels under passive conditions. Furthermore, myogenic tone developed similarly in vessels from either types of mice after distention in the presence of L-NAME (Fig. 4*A*). In contrast, myogenic tone in $MT^{-/-}$ vessels was significantly less than $MT^{+/+}$ vessels when endogenous NO was generated (Fig. 4*B*), as confirmed by its partial reversibility with L-arginine (Fig. 4*C*). Myogenic reflexes were similar in wild-type mice whether they were backbred or directly crossed between OLA129 and C57BL6. Therefore, the interaction between NO and MT facilitates this important vascular reflex.

Discussion

In this report, several genetic approaches were used, including a chimeric reporter molecule (FRET-MT) as well as MT knockout mice, to reveal a role for MT in NO signaling in vascular tissue. Accordingly, the current study provides several demonstrations of the technical potential of the chimera as well as a bioregulatory role of MT in mediating the effect of NO in resistance vessels.

FRET, MT, and NO. First, we demonstrate that FRET-MT can be used as an intracellular surrogate indicator of NO production (Figs. 2 and 3). Because this construct is encoded by a piece of cloned DNA, molecular strategies could be used to express FRET-MT in specific cell types including selective subcellular localization (13) in culture or even in particular tissues in transgenic animals. It is interesting to note that the persistence of the change in the FRET-MT signal in response to NO may facilitate assaying of many samples for drug screening or many optical sections for tissue physiology studies. To the best of our knowledge, this is the first demonstration of detection of conformational changes of a single native human protein by GFP-based FRET in intact cells and extends the approach originally described for the recombinant reporter cameleon (13) consisting of tandem fusions of mutated donor GFPs, calmodulin, calmodulin-binding peptide M13, and acceptor GFPs. Second, our results also prove that biological levels of NO generated in response to activation of endogenous receptors interacts with MT in live cells. Hence, the metal thiolate clusters of MT are likely to be an additional target for NO signaling in vascular and other tissue. Thus, in addition to the well known role of iron and/or cysteines as bioregulatory targets of NO (8), it appears that zinc-thiolate cluster of MT and perhaps other zinc-cysteine structures may also be involved in NO signaling. Previous reports have shown that exogenous NO can (*i*) increase intracellular levels of free zinc as detected by zinc-sensitive fluorescent probes in mouse fibroblasts (24); (*ii*) react with authentic MT *in vitro* leading to the release of zinc (9) or cadmium (10); and (*iii*) form stable EPR detectable complexes with MT having a signal consistent with mono- or dinitrosyl iron MT complex (11, 12). Based on our current results with FRET-MT (Figs. 1–3), it appears highly likely that NO (or some secondary nitrogen monoxide product) can react with MT in intact cells, resulting in an unfolding of MT and release of bound metal. This biochemical pathway may explain the protective role of MT against nitrosative stress we previously noted in NIH 3T3 cells (12) or the participation of MT in the myogenic reflex of murine mestenteric resistance arteries (Fig. 4).

Physiologic Function of MT: Role in NO-Mediated Signaling in Myogenic Reflex. Since its identification over 40 years ago, the function of MT has remained unclear (1–3). Two independent groups engineered null mutant mice for MT-I and MT-II, and surprisingly there was no identifiable phenotype of these mice under standard laboratory conditions (15, 25) except for a provocative (1), but unconfirmed, report that the animals became obese (26). These mice, however, were sensitive to cadmium-induced lethality (15, 25) as well as cadmium-induced liver (27) and renal (28) toxicity, leading to the conclusion that a major function of MT is to reduce the sensitivity to cadmium and other heavy metals (2). Nonetheless, it appears that MT has

evolved for other functions (1), and recent *in vitro* data suggest a novel role for the thiolate clusters of MT in intracellular redox regulation (4–7). Over-expression of MT protects cells (28, 29) and intact organs (30–32) against various forms of oxidative stress, and under-expression enhances the sensitivity of cells (33–35) to similar stimuli. From observations on partially purified MT *in vitro*, Maret and Vallee (4–7) recently reported that the zinc-thiolate clusters of MT are unique sites in that they are readily oxidized by a variety of agents, thereby conferring a kinetic liability (e.g., release of bound metals) to an otherwise thermodynamically stable complex. Thus, rather than viewing MT as an expendable target in cellular redox chemistry, these authors interpret their observations to indicate that the redox properties of the unique metal thiolate clusters in MT render this molecule as a potentially important component of intracellular signaling, facilitating the release or uptake of ions such as zinc secondary to alterations in cellular redox.

In this regard, the NO that is formed in response to increased intraluminal pressure appears to cause greater relaxation in $MT^{-/-}$ than $MT^{+/+}$ vessels (Fig. 4*B*), accounting for the L-NAME-sensitive lack of myogenic tone in $MT^{-/-}$ vessels (Fig. 4*A*). This enhanced relaxing effect of NO during myogenic reflex in $MT^{-/-}$ vessels may be direct (increased availability of NO to affect presumptive targets such as soluble guanylate cyclase or calcium activated potassium channels) or indirect (lack of releasable metals from MT that normally would produce contraction). Regardless of the precise molecular mechanism, the current study clearly identifies a role for constitutive levels of MT in mammalian NO-dependent physiology and suggests that MT may have fundamental roles in signal transduction by acting as a critical labile pool of releasable zinc and/or copper.

We thank Dr. Roger Tsien (University of California, San Diego) for the gift of the cDNA for cameleon and Dr. Jan Vilcek (New York University) for cDNA for hMT-IIa. $MT^{-/-}$ mice were generously provided by Drs. Anna Michalska and K. H. A. Choo. This work was supported in part by National Institutes of Health Grants HL-32154 and GM-53789 (B.R.P.), NS32385 and HL55312 (E.S.L), and HL-07563 (L.L.P.).

1. Palmiter, R. D. (1998) *Proc. Natl. Acad. Sci. USA* **95,** 8428–8430.
2. Lazo, J. S. & Pitt, B. R (1995) *Annu. Rev. Pharmacol. Toxicol.* **35,** 635–653.
3. Klaassen, C. D., Liu, J. & Choudhuri, S. (1999) *Annu. Rev. Pharmacol. Toxicol.* **39,** 267–294.
4. Maret, W. & Vallee, B. L. (1998) *Proc. Natl. Acad. Sci. USA* **95,** 3478–3482.
5. Jiang, L. J., Maret, W. & Vallee, B. L. (1998) *Proc. Natl. Acad. Sci. USA* **95,** 3483–3488.
6. Jacob, C., Maret, W. & Vallee, B. L. (1998) *Proc. Natl. Acad. Sci. USA* **95,** 3489–3494.
7. Maret, W., Jacob, C., Vallee, B. L. & Fischer, E. H. (1999) *Proc. Natl. Acad. Sci. USA* **96,** 1936–1940.
8. Stamler, J. S. (1994) *Cell* **78,** 931–936.
9. Kroncke, K. D., Fehsel, K., Schmidt, T., Zenke, F. T., Dasting, I., Wesener, J. R., Bettermann, H., Breuning, K. D. & Kolb-Bachofen, V. (1994) *Biochem. Biophys. Res. Commun.* **200,** 1105–1110.
10. Misra, R. R., Hochadel, J. F., Smith, G. T., Cook, J. C., Waalkes, M. P.& Wink, D. A. (1996) *Chem. Res. Toxicol.* **9,** 326–332.
11. Kennedy, M. C., Gan, T., Antholine, W. E. & Petering, D. H. (1993) *Biochem. Biophys. Res. Commun.* **196,** 632–635.
12. Schwarz, M. A., Lazo, J. S., Yalowich, J. C., Allen, W. P., Whitmore, M., Bergonia, H. A., Tzeng, E., Billiar, T. R., Robbins, P. D., Lancaster, J. R. & Pitt, B. R. (1995) *Proc. Natl. Acad. Sci. USA* **92,** 4452–4456.
13. Miyawaki, A., Llopis, J., Heim, R., McCaffrey, J. M., Adams, J. A., Ikura, M. & Tsien, R. Y. (1997) *Nature (London)* **388,** 882–887.
14. Hoyt, D. G., Mannix, R. J., Rusnak, J. M., Pitt, B. R. & Lazo, J. S. (1995) *Am. J. Physiol.* **269,** L171–L177.
15. Michalska, A. E. & Choo, K. H. A. (1993) *Proc. Natl. Acad. Sci. USA* **90,** 8088–8092.
16. Kanai, A. J., Strauss, H. C., Truskey, G. A., Crews, A. L., Grunfeld, S. & Malinski, T. (1995) *Circ. Res.* **77,** 284–293.
17. Gandley, R. E., Griggs, K. C., Conrad, K. P. & McLaughlin, M. K. (1997) *Am. J. Physiol.* **273,** R22–R27.
18. Eaton, D. L. & Toal, D. F. (1982) *Toxicol. Appl. Pharmacol.* **66,** 134–142.
19. dos Remedios, C. G. & Moes, P. D. (1995) *J. Struct. Biol.* **115,** 175–185.
20. Gordon, G. W., Berry, G., Liang, X. B., Levine, B. & Herman, B. (1998) *Biophys. J.* **74,** 2702–2713.
21. Winge, D. R. & Miklossy, K. A (1982) *J. Biol. Chem.* **257,** 3471–3476.
22. Lizasoain, I., Moro, M., Knowles, R., Darley-Usmar, V. & Moncada, S. (1996) *Biochem. J.* **314,** 877–880.
23. Osawa, M., Swindells, M. B., Tanikawa, J., Tanaka, T., Mase, T., Furuya, T. & Ikura, M. (1998) *J. Mol. Biol.* **276,** 165–176.
24. Berendji, D., Kolb-Bachofen, V., Meyer, K. L., Grapenthin, O., Weber, H., Wahn, V. & Kroncke, K.-D. (1997) *FEBS Lett.* **405,** 37–41.
25. Masters, B. A., Kelley, E. J., Quaife, C. J., Brinster, R. L. & Palmiter, R. D. (1994) *Proc. Natl. Acad. Sci USA* **91,** 584–588.
26. Beattie, J. H., Wood, A. M., Newman, A. M., Bremner, I., Choo, K. H. A., Michalska, A. E., Duncan, J. S. & Trayhurn, P. (1998) *Proc. Natl. Acad. Sci. USA* **95,** 358–363.
27. Liu, J., Liu, Y. P., Michalska, A. E., Choo, K. H. A. & Klaassen, C. D. (1996) *J. Pharmacol. Exp. Ther.* **276,** 1216–1223.
28. Tamei, K. T., Gralla, E. B., Ellerby, L. M., Valentine, J. S. & Thiele, D. J. (1993) *Proc. Natl. Acad. Sci. USA* **90,** 8013–8017.
29. Schwarz, M. A., Lazo, J. S., Yalowich, J. C., Reynolds, I., Kagan, V. E., Tyurin, V., Kim, Y.-M., Watkins, S. C. & Pitt, B. R. (1994) *J. Biol. Chem.* **269,** 15238–15242.
30. Kang, Y. J., Chen, Y., Voss-McCowan, M. & Epstein, P. N. (1997) *J. Clin. Invest.* **100,** 1501–1506.
31. Kang, Y. J., Li, G. & Saari, J. T. (1999) *Am. J. Physiol.* **276,** H993–H997.
32. Liu, J., Liu, Y., Hartley, D., Klaassen, C. D., Shehin-Johnson, S. E., Lucas, A. & Cohen, S. D. (1999) *J. Pharmacol. Exp. Ther.* **289,** 580–586.
33. Chubatsu, L. S. & Meneghini, R. (1994) *Biochem. J.* **291,** 193–198.
34. Lazo, J. S., Kondo, Y., Michalska, A., Choo, K. H. A. & Pitt, B. R. (1995) *J. Biol. Chem.* **270,** 5506–5510.
35. Kondo, Y., Rusnak, J. M., Hoyt, D. G., Settineri, C. E., Pitt, B. R. & Lazo, J. S. (1997) *Mol. Pharmacol.* **52,** 195–202.